NANO LETTERS

pubs.acs.org/NanoLett

Rapid Cytosolic Delivery of Luminescent Nanocrystals in Live Cells with Endosome-Disrupting Polymer Colloids

Andrea R. Bayles, Harvind S. Chahal, Dev S. Chahal, Cheryl P. Goldbeck, Bruce E. Cohen, and Brett A. Helms*

The Molecular Foundry, Lawrence Berkeley National Laboratory, 1 Cyclotron Road, Berkeley, California 94720

ABSTRACT Luminescent nanocrystals hold great potential for bioimaging because of their exceptional optical properties, but their use in live cells has been limited. When nanocrystals enter live cells, they are taken up in vesicles. This vesicular sequestration is persistent and precludes nanocrystals from reaching intracellular targets. Here, we describe a unique, cationic core−shell polymer colloid that translocates nanocrystals to the cytosol by disrupting endosomal membranes via a low-pH triggered mechanism. Confocal fluorescence microscopy and flow cytometry indicate that picomolar concentrations of quantum dots are sufficient for cytosolic labeling, with the process occurring within a few hours of incubation. We anticipate a host of advanced applications arising from efficient cytosolic delivery of nanocrystal imaging probes: from single particle tracking experiments to monitoring protein−protein interactions in live cells for extended periods.

KEYWORDS Nanocrystal, delivery, bioimaging, endosomal disruption, live cell microscopy

Intracellular signaling pathways have proved to be enormously complex, and dissecting them is a major focus in cell[1] and cancer[2] biology. Multiplexed analysis of these processes with spatiotemporal resolution in live cells has been limited to the extent to which fluorescent or luminescent probes remain active and bright during the observation period, which can last from several hours up to days. Owing to their exceptionally stable optical properties, luminescent nanocrystals have emerged as near ideal reagents for molecular level imaging of biological events in individual cells.[3] One of the major challenges in applying them as probes for cellular imaging, however, has been the difficulty of using them inside of live cells.[4] Nanocrystals are typically taken up by live cells via endocytosis and the large majority remains trapped in endosomes, unable to reach the cytosol.[5] Staining patterns corresponding to one or more nanocrystals confined to endosomes are characteristically punctate and often bright enough to obscure nanocrystal luminescence elsewhere in the cytosol from those that may have adventitiously escaped. Nanocrystals have been directly introduced into the cytosol using microinjection or electroporation; although, these methods are exceptionally labor intensive, low throughput, and frequently incur cell death or stress. Passive delivery strategies, including those mediated by polymers (e.g., lipofectamine or PLGA[4e]) or nanocrystal surface passivation with cell-penetrating peptides (e.g., the TAT peptide derived from HIV-1), have demonstrated some decrease in endosomal staining; however, the process is slow and the prevalence of residual puncta may still interfere with sensitive imaging experiments.[6] To develop an efficient and general method for targeting nanocrystals to the cytosol and subcellular organelles, we have synthesized proton sponge based core−shell polymer colloids that are able to bind nanocrystals, transport them into the cell, and release them into the cytosol within a few hours of application (Figure 1a). Furthermore, we find that picomolar concentrations of quantum dots bound to these colloids are sufficient to give good cytosolic luminescence, with minimal evidence of residual endosomal staining patterns. The overall process is both straightforward and general to a broad range of nanocrystal-based probe designs. We expect the technique to substantially simplify how researchers apply nanocrystals for imaging and diagnostics in live cells.

Noting that membrane impermeability and endosomal sequestration prevent nanocrystals from reaching the cytosol of live intact cells, we hypothesized that delivery could be conferred if endosomal disruption were to be triggered by some physical or chemical stimulus. pH-responsive polymer colloids have previously been shown to mediate the delivery of membrane impermeable macromolecules—including drugs, proteins, and nucleic acids—to intracellular targets in phagocytic dendritic cells and macrophages by facilitating endocytosis and then disrupting late endosomes at low intraorganelle pH (ca. 5.0−5.5).[7] For example, acetalated dextran-based colloids[8] (Ac-Dex) undergo pH-triggered decomposition in endolysosomal compartments, putatively resulting in osmotic shock and endosomal rupture, while colloids comprised of proton sponges[9]—e.g., poly(β-amino esters)[10] (PBAEs)—do so presumably via electrostatic destabilization of the membrane. An initial screen of micropar-

* To whom correspondence should be addressed, bahelms@lbl.gov.
Received for review: 06/21/2010
Published on Web: 09/10/2010

© 2010 American Chemical Society

DOI: 10.1021/nl102172j | *Nano Lett.* **2010,** *10,* 4086–4092

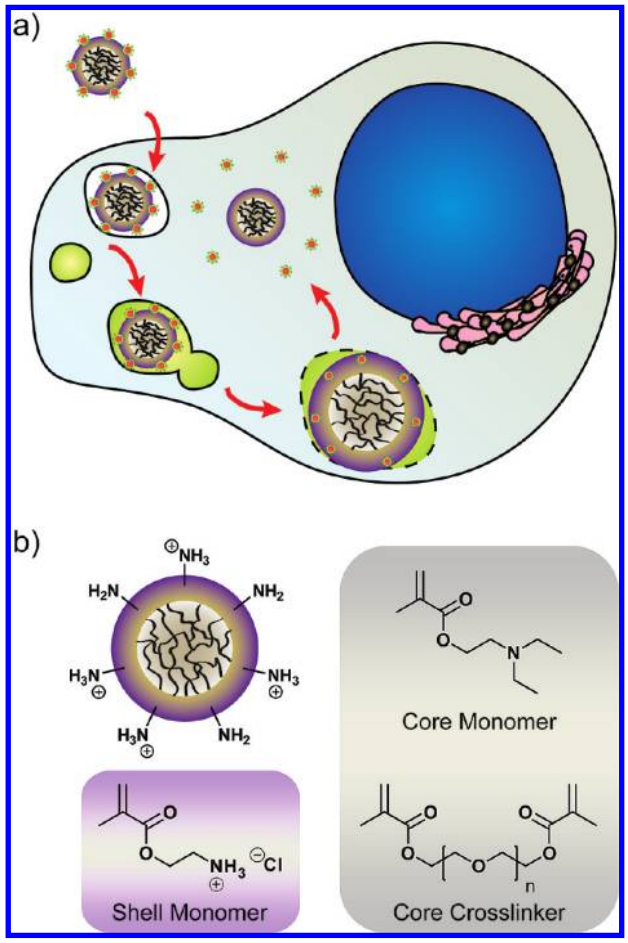

FIGURE 1. Delivery of nanocrystals to the cytosol of live cells with cationic core−shell polymer colloids. (a) Suggested mechanism of cellular uptake, trafficking, expansion, and endosomal rupture, leading to cytosolic delivery of nanocrystals. (b) Schematic depiction of cationic core−shell polymer colloids and their constituent monomers.

ticulate colloids (diameters ~250 nm) prepared from these polymers and their blends as delivery agents for protein-coated CdSe/ZnS core−shell quantum dots (QDs) to HeLa cells, which are a nonphagocytic cell line, showed either weak staining, suggestive of poor cellular uptake, or puncta, suggestive of sequestration within endosomes (panels a and b of Figure 2, respectively). Other formulations along these lines from acid degradable polyurethanes and acid degradable PBAEs were likewise poor delivery agents or had little propensity for nanocrystal adsorption (data not shown). We concluded that charge-neutral colloids, as prepared from Ac-Dex or acid degradable polyurethanes, were not efficient carriers of nanocrystals to nonphagocytic cell types. Furthermore, when the surface potential of these polymer vectors was manipulated to have partial cationic character, e.g., via blending of Ac-Dex with 10% w/w PBAEs, the internalization efficiency improved; however, the intracellular trafficking pathways seem not to give rise to the same low-pH-driven endolysosomal release pathways that is typically observed for phagocytic cell types. Our results are consistent with recent work pointing to the importance of both cell type (i.e., phagocytic versus nonphagocytic) and colloid surface charge in mediating efficient uptake and cytosolic delivery of macromolecular cargo.[11] Thus, while there are many lessons to glean from the vast literature on polymer carriers of membrane impermeable macromolecular cargo, most have not demonstrated broad applicability to nonphagocytic cell types (i.e., the majority of cells) nor have any demonstrated efficient delivery of nanocrystals to the cytosol of live cells, free from endosomal confinement, which is a prerequisite for most advanced bioimaging schemes.

In an effort to develop a more efficient and general method for the delivery of nanocrystals to the cytosol of nonphagocytic cells, we designed cationic core−shell polymer colloids containing a pH-buffering proton sponge using poly(ethylene glycol) dimethacrylate (PEGDMA, MW = 330 Da) cross-linked poly(2-(diethylamino)ethyl methacrylate) (PDEAEMA) for the core and poly(2-aminoethyl methacrylate) (PAEMA) for the shell (Figure 1b). The colloids were synthesized by surfactant-free emulsion polymerization at 70 °C in water using ammonium persulfate (APS) as the initiator. The PDEAEMA-*co*-PEGDMA cross-linked proton sponge cores were grown for 3 h, reaching a diameter of ~120 nm, prior to the addition of AEMA for the shell. Colloids were purified by dialysis and characterized by dynamic light scattering (DLS) at physiologically relevant neutral and acidic pH (Figure S2 in the Supporting Information). Independent of temperature, these colloids expand dramatically below pH 6, exhibiting up to a 50-fold increase in volume, consistent with recent studies of related hydrogels.[12] This is a direct consequence of the proton sponge core, which becomes charged and solvated at low pH as the PDEAEMA's tertiary amines become protonated. We and others have demonstrated that the volume expansion exhibited by these cationic core−shell polymer colloids disrupts late endosomal membranes,[12,12e] possibly providing for a novel mechanism of release for bound nanocrystals into the cytosol of live cells. The increase in volume is concomitant with an increase in the ζ potential from +7 mV at pH 7.4 to +45 mV at pH 5.5, which may also serve to compromise endosomal membrane integrity in a manner similar to PBAEs. To the best of our knowledge, cationic core−shell colloids such as these have not been employed previously to deliver nanocrystals to the cytosol of live cells nor have they demonstrated applicability to nonphagocytic cells types as described here.

Addition of streptavidin-coated quantum dots (605-SA-QDs, diameter ~20 nm, λ_{em} = 605 nm, ζ = −9 mV in PBS at pH 7.4) to the colloids led to facile self-assembly, presumably through multivalent electrostatic interactions between the ammonium ions on the colloid shell and acidic streptavidin side chains (Scheme 1). After 12 h, the coassembly showed a monomodal distribution by DLS and, most importantly, quantum dot luminescence was undiminished

© 2010 American Chemical Society

DOI: 10.1021/nl102172j | *Nano Lett.* **2010,** *10,* 4086–4092

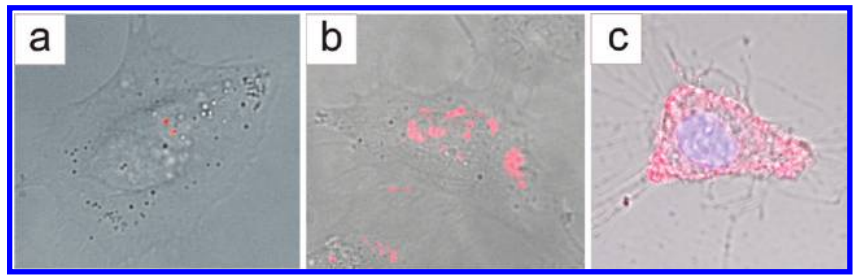

FIGURE 2. Vector-mediated internalization of 605-SA-QDs (5 nM) by HeLa cells using various pH-responsive polymer colloids. Nanocrystal staining patterns were observed using wide-field fluorescence microscopy. Bright field images are shown for three vectors with the nanocrystal channel overlaid in order to visualize the fate of nanocrystals using the different chemical compositions and thus mechanisms for delivery. Acid degradable Ac-Dex based vectors (a) gave weak signals in the 605-SA-QD channel suggesting poor internalization efficiency for this cell type. Improved cell uptake was observed for vectors comprised of Ac-Dex blended with 10% w/w PBAEs (b); however the staining pattern was characteristically punctuate suggesting vesicular confinement. In contrast, cationic PDEAEMA-*co*-PEGDMA core−PAEMA shell polymer vectors with low pH-mediated volume expansion showed diffuse cytosolic staining (c) suggesting nanocrystals no longer reside in vesicles.

SCHEME 1. Adsorption of Anionic Streptavidin-Coated Quantum Dots onto the Surface of Cationic Core−Shell Polymer Colloids via Nonspecific Electrostatic Interactions

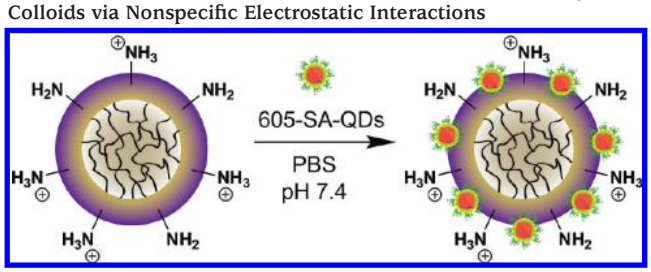

(data not shown). Increasing the ratio of quantum dots to colloids resulted in a monotonic increase in the diameter of the assembly, from 155 to 180 nm, with an inversion of the ζ potential to negative values observed for quantum dot concentrations exceeding 5 nM (Figure 3). We anticipated that the internalization of quantum dot loaded colloids would be optimal when the overall ζ potential at the surface remained positive. Furthermore, initial cell viability assays (Figure S4 in the Supporting Information) indicated that cell health was adversely affected for colloid concentrations in excess of 100 μg mL^{-1}. Therefore, we proceeded with cell labeling experiments with no greater than 100 μg mL^{-1} of the colloids used in conjunction with less than 5 nM of the streptavidin-coated quantum dots.

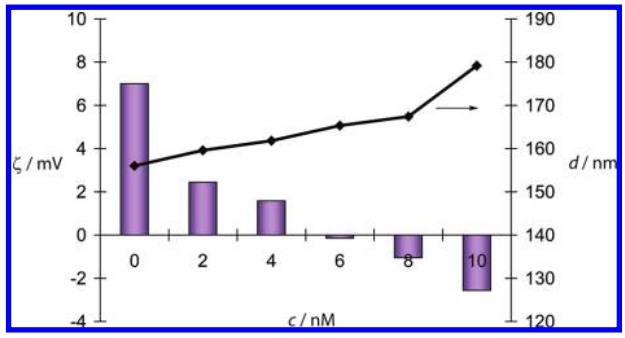

FIGURE 3. Changes in surface potential (ζ) and diameter (d) of cationic core−shell polymer colloids charged with QDs in PBS at pH 7.4 at the indicated concentrations (c) as determined by electrokinetic potential measurements and dynamic light scattering.

For live cell imaging, HeLa cells were incubated with 50−100 μg mL^{-1} of cationic polymeric colloids coated with quantum dots or with an equivalent concentration of quantum dots alone. In contrast to charge neutral colloids based on acetalated dextrans or their blends with PBAEs, cells incubated with quantum dot loaded (PDEAEMA-*co*-PEGDMA)-*graft*-PAEMA core−shell colloids showed diffuse luminescence in the cytosol after as little as 4 h (Figure 2C). Rapid delivery appears to be characteristic for these colloids over other polymer carriers, which often require between 24 and 48 h to disrupt endosomes.[4e,8,10] Potential mechanisms for this colloid-mediated endosomal disruption are being explored and include mechanical breach of endosomal bilayers by explosive colloid expansion, osmotic shock caused by hydration of cations within the previously hydrophobic core, or rapid changes electrochemical potential due to the movement of anions to the core.

The extent to which the cationic polymer colloids affected the subcellular localization of internalized quantum dots was investigated with confocal fluorescence microscopy and colocalization with known organelle stains. In these experiments, HeLa cells were exposed to the lipophilic membrane tracer dye 3,3′-dioctadecyloxacarbocyanine perchlorate (DiO, λ_{em} = 501 nm) to visualize endosomes, as well as the nuclear stain 4′,6-diamidino-2-phenylindole (DAPI, λ_{em} = 461 nm). In control experiments without the polymer colloids, we did not observe accumulation of quantum dots in HeLa cells at subnanomolar concentrations (Figure 4a−c); although endosomes were readily observed as indicated by the punctate staining pattern in the DiO channel (Figure 4a,c, green). This points to the efficacy with which our DiO-based staining protocol allows for the visualization of endosomes over the time period of nanocrystal entry to the cell. At higher concentrations of quantum dots (e.g., 5 nM), their internalization was pronounced but confined to vesicular compartments, as evidenced by strong colocalization in the DiO and 605-SA-QD signals (Figure S5, yellow (Supporting Information)). This endosomal sequestration persisted even after 12 h following incubation, indicating relatively little self-mediated escape or disruption of endosomal membranes by

© 2010 American Chemical Society

DOI: 10.1021/nl102172j | *Nano Lett.* **2010,** *10,* 4086–4092

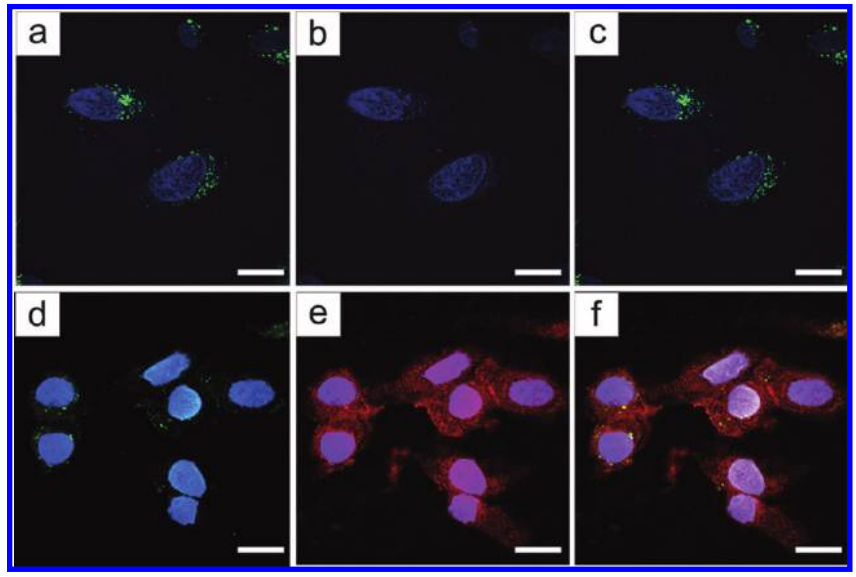

FIGURE 4. Confocal fluorescence microscopy determines the intracellular fate of nanocrystals delivered to live HeLa cells. HeLa cells incubated with 500 pM 605-SA-QDs in the absence of polymeric colloids show poor labeling efficiency: (a) nuclear (DAPI) and endosomal (DiO) fluorescence; (b) nuclear and QD signals; (c) an overlay of these two images. HeLa cells incubated with 500 pM 605-SA-QDs in the presence of polymer colloids, on the other hand, show a high degree of cytosolic labeling without residual punctuate endosomal staining patterns: (d) nuclear and endosomal fluorescence; (e) nuclear and QD signals; (f) an overlay of these two images. All images were captured and processed identically, as described in the Supporting Information. Scale bar is 5 μm.

the quantum dots themselves. In contrast, the cationic polymer colloid mediated delivery of quantum dots featured both intense and diffuse perinuclear staining patterns as well as weak colocalization with DiO labeled endosomes (Figure 4d−f). Instances where strong DiO colocalization was observed with quantum dots (Figure 4f, yellow) suggest a scant fraction of endosomes are slow to acidify. Shorter incubation times or lower concentrations of quantum dots both gave less intense labeling in the cytosol, offering an efficient means of controlling the number of nanocrystals introduced into cells for single particle tracking and other applications where a low degree of labeling is desirable.

Insight into the mechanism of cytosolic delivery was carried out by visualizing quantum dot distribution in HeLa cells as a function of time following incubation with the colloid−quantum dot assemblies. Live HeLa cells were treated with 605-SA-QDs (1 nM) bound to our cationic core−shell polymer colloids (50 μg mL^{-1}) for 1 h. Cells were then washed extensively, and fresh growth medium was introduced before further incubation at 37 °C. After various time points (4, 8, 12, and 24 h) following the initial incubation, the subcellular localization of the 605-SA-QDs was investigated using confocal fluorescence microscopy. As before, endosomal (DiO) and nuclear (DAPI) stains were applied so that residual confinement of 605-SA-QDs to endosomes could be visualized directly. Internalization of 605-SA-QDs bound to polymer colloids was rapid (Figure 5a−c), with pronounced luminescence after 1 h. Some colocalization between 605-SA-QDs and DiO-labeled endosomes was observable immediately following the incubation (Figure 5C), although the majority of particles appear to have already escaped vesicular confinement. At this stage of the delivery, nanocrystals remain bound to the polymer colloids, which give rise to slightly larger staining features (Figure 5B). After 4 or 8 h, the nanocrystal staining patterns were more diffuse throughout the cytosol (Figure 5d−f). No colocalization with DiO labeled endosomes was observable at these and later stages (Figure 5g−i). Diffuse cytosolic staining was persistent even after 24 h (Figure 5j−l), with cell densities and morphologies phenomenologically consistent with earlier times. Some nanocrystal aggregation can be inferred from the images taken at 24 h, which may point to a future effort in more stable coatings for nanocrystals used in intracellular work. Nevertheless, the protocol appears to meet the demands for nanocrystal imaging over extended periods with cells in culture. The imaging results also suggest that the rate-limiting step in the delivery scheme is likely to be the diffusion of nanocrystals from the polymer colloids. Optimized chemistries at the colloid-nanocrystal interface to control this process in cells are currently being explored.

While fluorescence images are a critical gauge of cellular labeling techniques, variations in cell type, microscope settings, image processing, and interpretation make quantitative comparisons difficult. Therefore, we employed flow cytometry to quantify the labeling efficiency and possible toxicity imparted by the cationic polymer colloid or the quantum dots themselves. HeLa cells were incubated with quantum dots either in the absence or in the presence of the polymer vector as in previous experiments. In the absence of the polymer vector, there was no increase in 605 nm emission over background in cells treated with 50 or 500 pM quantum dots alone (Figure 6a), in good agreement with the confocal fluorescence microscopy experiments that pointed to poor internalization efficiency at subnanomolar

© 2010 American Chemical Society

DOI: 10.1021/nl102172j | *Nano Lett.* **2010,** *10,* 4086–4092

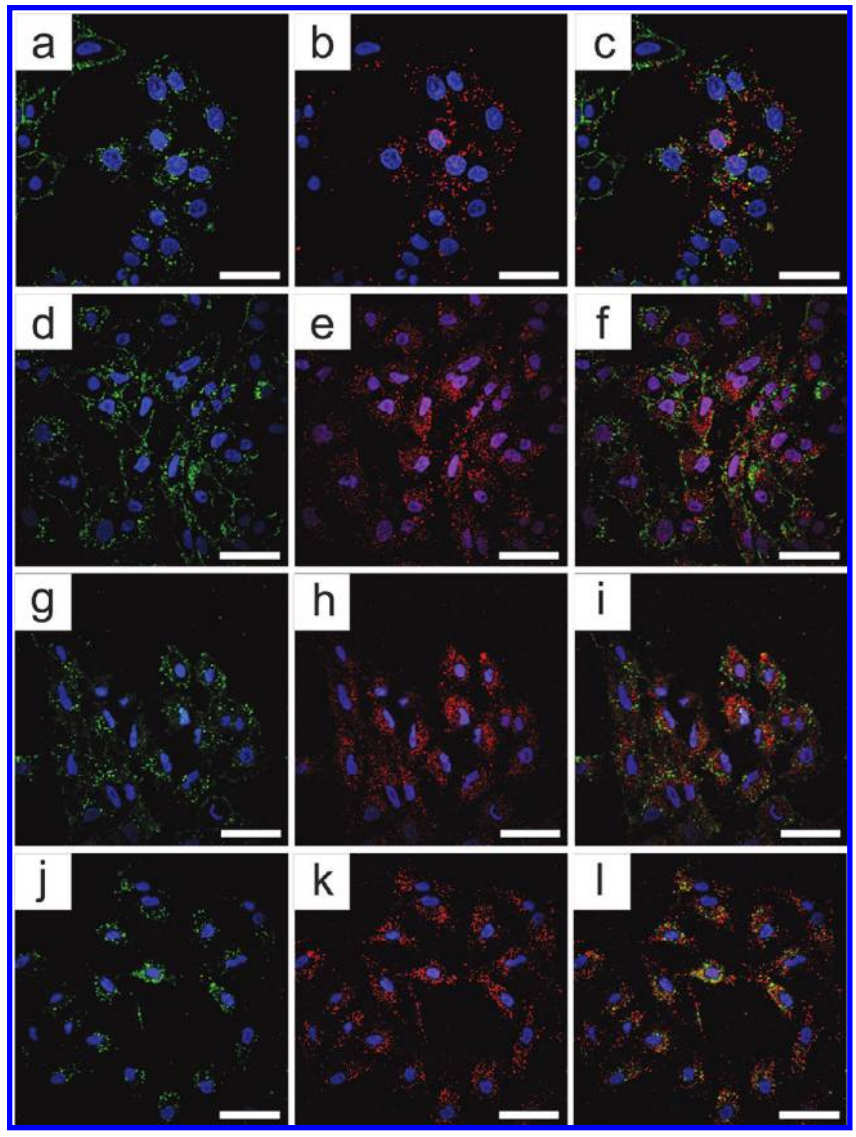

FIGURE 5. Dynamics and mechanistic aspects of vector-mediated nanocrystal delivery to the cytosol. Confocal fluorescence microscopy of HeLa cells incubated with 605-SA-QDs (1 nM) and cationic core−shell polymer colloids (50 ug mL^{-1}) was carried out. After an initial incubation of 1 h, cells were washed extensively and subsequently imaged at different time points during the delivery process: 0 h (a−c), 8 h (d−f), 12 h (g−i), and 24 h (j−l). Nuclei were stained with DAPI (blue) with membranes and endosomes stained by DiO (green). Key: (a, d, g, and j) nuclear and endosomal fluorescence; (b, e, h, and k) nuclear and QD signals; and (c, f, i, and l) an overlay of these two images. Colocalization of cationic core−shell polymer colloids loaded with 605-SA-QDs (yellow) appeared primarily after the initial incubation (c), while characteristic diffuse cytosolic labeling occurred in 4−8 h. All images were captured and processed identically, as described in the Supporting Information. Scale bar is 25 μm.

concentrations of probes. At a quantum dot concentration of 5 nM, labeling was clearly observed, with the increase in the geometric mean fluorescence 2.5-fold above background (Figure 6a, purple), although the confocal fluorescence imaging indicates that the probes remained sequestered in endosomes under these labeling conditions (Figure S5 in the Supporting Information). By comparison, the quantum dot delivery efficiency to HeLa cells was markedly improved in the presence of polymer colloids, and the extent of labeling was commensurate with increasing concentrations of the probes. In the highest concentration tested (5 nM), the increase in the geometric mean fluorescence above background was approximately 20-fold. These results were also consistent with the confocal fluorescence microscopy experiments where the degree of cytosolic staining was determined by the initial concentration of the probes and to a lesser extent the incubation time.

As a preliminary, qualitative measure of toxicity, the scatter plots from the flow cytometry experiments indicated that the presence of increasing amounts of quantum dots in the cytosol led to a decrease in both the average size of the HeLa cells and the degree of internal complexity (or granularity—e.g., fewer subcellular compartments, including endosomes), suggesting that the directed cytosolic delivery of these particular quantum dots to live cells had a pronounced effect on cell physiology (Figure S6 in the Support-

© 2010 American Chemical Society

DOI: 10.1021/nl102172j | *Nano Lett.* **2010,** *10,* 4086–4092

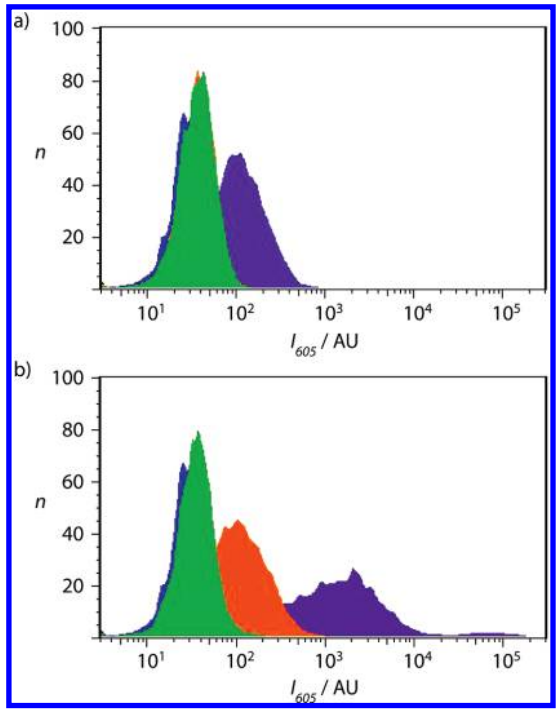

FIGURE 6. Quantitative assessment of nanoparticle uptake by flow cytometry of HeLa cells incubated with 605-SA-QDs or 605-SA-QD/polymer colloids: (a) HeLa cells alone (blue), incubated with 50 pM (green), 500 pM (orange, mostly obscured), or 5 nM (purple) 605-SA-QDs; (b) cells alone (blue), incubated with 50 pM (green), 500 pM (orange), or 5 nM (purple) 605-SA-QD/polymer colloids. The distributions reflect the number of cells (n) with a given luminescence intensity (I_{605}) and are reported for a representative sampling of 10000 cells for each measurement.

ing Information). In control experiments, neither colloid alone nor quantum dots alone showed similar effects. Previous work has not yielded a consensus on nanocrystal cell toxicity or its possible origins,[13] which may arise from phenomena as varied as heavy metal leaching from the nanocrystal, specific physiological responses to the quantum dot surface coatings, or the nature of synthetic nanomaterials themselves. These initial results point to the opportunity to use these cationic polymer vectors in conjunction with flow cytometry as well as genomic and proteomic analyses to establish how and to what extent these luminescent nanocrystals affect specific aspects of cell biology. Given the efficiency of delivery for nanometer-scale objects to the cytosol as shown here, other nanoparticles may also be explored for their toxicity and downstream effects on cell physiology.

For live cell imaging with quantum dots and other nanoscale probes, their complacent sequestration in vesicles has been commonplace and a persistent challenge to overcome. We have shown here that quantitative release from endosomes is afforded by first assembling them to our pH-responsive cationic core−shell polymer colloids before introducing them to cells. The process is technically very simple and affords cytosolic delivery in only a few hours after incubation. The methodology is demonstrated for a nonphagocytic cell line, which is generally recognized to be more difficult, granting researchers the option of pursuing multiplexed imaging experiments with a broader range of cells. As it is amenable to high throughput schemes, we envision a myriad of possible applications in cell and cancer biology, nanomedicine, and medical diagnostics. The efficiency of delivery also suggests that these colloids should be useful in addressing nagging questions about nanocrystal toxicity to cells.

Acknowledgment. We thank Joel Cohen, Eric Bachelder, and Jean M. J. Fréchet for technical assistance and helpful discussions with this paper and Holly Aaron of the Molecular Imaging Center at the University of California, Berkeley for microscope access and advice. Work at the Molecular Foundry was supported by the Director, Office of Science, Office of Basic Energy Sciences, Division of Materials Sciences and Engineering, of the U.S. Department of Energy under Contract No. DE-AC02-05CH11231.

Supporting Information Available. Complete synthesis methods, characterization tools, and imaging protocols. This material is available free of charge via the Internet at http://pubs.acs.org.

REFERENCES AND NOTES

(1) (a) Berridge, M. J.; Lipp, P.; Bootman, M. D. *Nat. Rev. Mol. Cell Biol.* **2000**, *1*, 11. (b) Zhang, J.; Campbell, R. E.; Ting, A. Y.; Tsien, R. Y. *Nat. Rev. Mol. Cell Biol.* **2002**, *3*, 906. (c) Jan, L. Y.; Siegelbaum, S. A. *Curr. Opin. Neurobiol.* **2005**, *15*, 253. (d) Jørgensen, C.; Linding, R. *Curr. Opin. Genet. Dev.* **2010**, *20*, 15. (e) Lee, K. H.; Lee, S.; Lee, W. Y.; Yang, H. W.; Heo, W. D. *Proc. Natl. Acad. Sci. U.S.A.* **2010**, *107*, 3412.

(2) (a) Yarden, Y.; Sliwkowski, M. X. *Nat. Rev. Mol. Cell Biol.* **2001**, *2*, 127. (b) Wu, X.; Liu, H.; Liu, J.; Haley, K. N.; Treadway, J. A.; Larson, J. P.; Ge, N.; Peale, F.; Bruchez, M. P. *Nat. Biotechnol.* **2003**, *21*, 41. (c) Gao, X.; Cui, Y.; Levenson, R. M.; Chung, L. W. K.; Nie, S. *Nat. Biotechnol.* **2004**, *22*, 969.

(3) (a) Alivisatos, A. P. *Science* **1996**, *271*, 933. (b) Bruchez, M.; Moronne, M.; Gin, P.; Weiss, S.; Alivisatos, A. P. *Science* **1998**, *281*, 2013. (c) Chan, W. C. W.; Nie, S. *Science* **1998**, *281*, 2016. (d) Michalet, X.; Pinaud, F.; Lacoste, T. D.; Dahan, M.; Bruchez, M. P.; Alivisatos, A. P.; Mitchell, P. *Nat. Biotechnol.* **2001**, *19*, 1013. (e) Michalet, X.; Pinaud, F.; Lacoste, T. D.; Dahan, M.; Bruchez, M. P.; Alivisatos, A. P.; Weiss, S. *Single Mol.* **2001**, *2*, 261. (f) Parak, W. J.; Gerion, D.; Pellegrino, T.; Zanchet, D.; Micheel, C.; Williams, S. C.; Boudreau, R.; Gros, M. A. L.; Larabell, C. A.; Alivisatos, A. P. *Nanotechnology* **2003**, *14*, R15. (g) Alivisatos, A. P. *Nat. Biotechnol.* **2004**, *22*, 47. (h) So, M.-K.; Xu, C.; Loening, A. M.; Gambhir, S. S.; Rao, J. *Nat. Biotechnol.* **2006**, *24*, 339. (i) Weissleder, R.; Kelly, K.; Sun, E. Y.; Shtatland, T.; Josephson, L. *Nat. Biotechnol.* **2005**, *23*, 1418. (j) Somers, R. C.; Bawendi, M. G.; Nocera, D. G. *Chem. Soc. Rev.* **2007**, *36*, 579. (k) Resch-Genger, U.; Grabolle, M.; Cavaliere-Jaricot, S.; Nitschke, R.; Nann, T. *Nat. Methods* **2008**, *5*, 763.

(4) (a) Stephens, D. J.; Pepperkok, R. *Proc. Natl. Acad. Sci. U.S.A.* **2001**, *98*, 4295. (b) Michalet, X.; Pinaud, F. F.; Bentolila, L. A.; Tsay, J. M.; Doose, S.; Li, J. J.; Sundaresan, G.; Wu, A. M.; Gambhir, S. S.; Weiss, S. *Science* **2005**, *307*, 538. (c) Chen, X.; Kis, A.; Zettl, A.; Bertozzi, C. R. *Proc. Nat. Acad. Sci. U.S.A.* **2007**, *104*, 8218. (d) Ruan, G.; Agrawal, A.; Marcus, A. I.; Nie, S. *J. Am. Chem. Soc.* **2007**, *129*, 14759. (e) Kim, B. Y. S.; Jiang, W.; Oreopoulos, J.; Yip, C. M.; Rutka, J. T.; Chan, W. C. W. *Nano Lett.* **2008**, *8*, 3887.

(5) Brandenburg, B.; Zhuang, X. *Nat. Rev. Microbiol.* **2007**, *5*, 197.

(6) (a) Jaiswal, J. K.; Mattoussi, H.; Mauro, J. M.; Simon, S. M. *Nat. Biotechnol.* **2003**, *21*, 47. (b) Derfus, A. M.; Chan, W.; Bhatia, S.

© 2010 American Chemical Society

DOI: 10.1021/nl102172j | *Nano Lett.* **2010,** *10,* 4086–4092

Adv. Mater. **2004**, *16*, 961. (c) Rozenzhak, S. M.; Kadakia, M. P.; Caserta, T. M.; Westbrook, T. R.; Stone, M. O.; Naik, R. R. *Chem. Commun.* **2005**, 2217. (d) Delehanty, J. B.; Medintz, I. L.; Pons, T.; Brunel, F. M.; Dawson, P. E.; Mattoussi, H. *Bioconjugate Chem.* **2006**, *17*, 920. (e) Duan, H.; Nie, S. *J. Am. Chem. Soc.* **2007**, *129*, 3333. (f) Ruan, G.; Agrawal, A.; Marcus, A. I.; Nie, S. *J. Am. Chem. Soc.* **2007**, *129*, 14759. (g) Medintz, I. L.; Pons, T.; Delehanty, J. B.; Susumu, K.; Brunel, F. M.; Dawson, P. E.; Mattoussi, H. *Bioconjugate Chem.* **2008**, *19*, 1785. (h) Joo, K.; Lei, Y.; Lee, C.; Lo, J.; Xie, J.; Hamm-Alvarez, S. F.; Wang, P. *ACS Nano* **2008**, *2*, 1553. (i) Rajan, S. S.; Liu, H. Y.; Vu, T. Q. *ACS Nano* **2008**, *2*, 153. (j) Qi, L.; Gao, X. *ACS Nano* **2008**, *2*, 1403. (k) Anas, A.; Okuda, T.; Kawashima, N.; Nakayama, K.; Itoh, T.; Ishikawa, M.; Biju, V. *ACS Nano* **2009**, *3*, 2419. (l) Wu, S.; Han, G.; Milliron, D. J.; Aloni, S.; Altoe, V.; Talapin, D. V.; Cohen, B. E.; Schuck, P. J. *Proc. Natl. Acad. Sci. U.S.A.* **2009**, *106*, 10917.

(7) (a) Bachelder, E. M.; Beaudette, T. T.; Broaders, K. E.; Paramonov, S. E.; Dashe, J.; Fréchet, J. M. J. *Mol. Pharmaceutics* **2008**, *5*, 876. (b) Paramonov, S. E.; Bachelder, E. M.; Beaudette, T. T.; Standley, S. M.; Lee, C. C.; Dashe, J.; Fréchet, J. M. J. *Bioconjugate Chem.* **2008**, *19*, 911.

(8) (a) Bachelder, E. M.; Beaudette, T. T.; Broaders, K. E.; Dashe, J.; Fréchet, J. M. J. *J. Am. Chem. Soc.* **2008**, *130*, 10494. (b) Broaders, K. E.; Cohen, J. A.; Beaudette, T. T.; Bachelder, E. M.; Fréchet, J. M. J. *Proc. Natl. Acad. Sci. U.S.A.* **2009**, *106*, 5497.

(9) (a) Lynn, D. M.; Anderson, D. G.; Putnam, D.; Langer, R. *J. Am. Chem. Soc.* **2001**, *123*, 8155. (b) Akinc, A.; Anderson, D. G.; Lynn, D. M.; Langer, R. *Bioconjugate Chem.* **2003**, *14*, 979. (c) Duan, H.; Nie, S. *J. Am. Chem. Soc.* **2007**, *129*, 3333. (d) Yezhelyev, M. V.; Qi, L.; O'Regan, R. M.; Nie, S.; Gao, X. *J. Am. Chem. Soc.* **2008**, *130*, 9006.

(10) (a) Lynn, D. M.; Langer, R. *J. Am. Chem. Soc.* **2000**, *122*, 10761. (b) Akinc, A.; Lynn, D. M.; Anderson, D. G.; Langer, R. *J. Am. Chem. Soc.* **2003**, *125*, 5316.

(11) (a) Davda, J.; Labhasetwar, V. *Int. J. Pharm.* **2002**, *233*, 51. (b) Fischer, D.; Li, Y.; Ahlemeyer, B.; Krieglstein, J.; Kissel, T. *Biomaterials* **2003**, *24*, 1121. (c) Hong, S.; Bielinska, A. U.; Mecke, A.; Keszler, B.; Beals, J. L.; Shi, X.; Balogh, L.; Orr, B. G.; Baker, J. R.; Banaszak Holl, M. M. *Bioconjugate Chem.* **2004**, *15*, 774. (d) Bçma, D.; Freivalds, T.; Buikis, I.; Harju, L. in *14th Nordic-Baltic Conference on Biomedical Engineering and Medical Physics*. 2008, pp 598−601. (e) Zhang, X.; Jin, Y.; Plummer, M. R.; Pooyan, S.; Gunaseelan, S.; Sinko, P. J. *Mol. Pharmaceutics* **2009**, *6*, 836. (f) Zhang, S.; Li, J.; Lykotrafitis, G.; Bao, G.; Suresh, S. *Adv. Mater.* **2009**, *21*, 419. (g) Beaudette, T. T.; Cohen, J. A.; Bachelder, E. M.; Broaders, K. E.; Cohen, J. L.; Engleman, E. G.; Fréchet, J. M. J. *J. Am. Chem. Soc.* **2009**, *131*, 10360. (h) Scita, G.; Di Fiore, P. P. *Nature* **2010**, *463*, 464.

(12) (a) Amalvy, J. I.; Unali, G.; Li, Y.; Granger-Bevan, S.; Armes, S. P.; Binks, B. P.; Rodrigues, J. A.; Whitby, C. P. *Langmuir* **2004**, *20*, 4345. Amalvy, J. I.; Wanless, E. J.; Li, Y.; Michailidou, V.; Armes, S. P.; Duccini, Y. *Langmuir* **2004**, *20*, 8992. Hu, Y.; Litwin, T.; Nagaraja, A. R.; Kwong, B.; Katz, J.; Watson, N.; Irvine, D. J. *Nano Lett.* **2007**, *7*, 3056. (d) You, J.-O.; Auguste, D. T. *Nano Lett.* **2009**, *9*, 4467. (e) Hu, Y.; Atukorale, P. U.; Lu, J. J.; Moon, J. J.; Um, S. H.; Cho, E. C.; Wang, Y.; Chen, J.; Irvine, D. J. *Biomacromolecules* **2009**, *10*, 756.

(13) (a) Derfus, A. M.; Chan, W. C. W.; Bhatia, S. N. *Nano Lett.* **2004**, *4*, 11. (b) Hoshino, A.; Fujioka, K.; Oku, T.; Suga, M.; Sasaki, Y. F.; Ohta, T.; Yasuhara, M.; Suzuki, K.; Yamamoto, K. *Nano Lett.* **2004**, *4*, 2163. (c) Lovriæ, J.; Cho, S. J.; Winnik, F. M.; Maysinger, D. *Chem. Biol.* **2005**, *12*, 1227. (d) Kirchner, C.; Liedl, T.; Kudera, S.; Pellegrino, T.; Javier, A. M.; Gaub, H. E.; Stölzle, S.; Fertig, N.; Parak, W. J. *Nano Lett.* **2005**, *5*, 331. (e) Ryman-Rasmussen, J. P.; Riviere, J. E.; Monteiro-Riviere, N. A. *Nano Lett.* **2007**, *7*, 1344.

© 2010 American Chemical Society

DOI: 10.1021/nl102172j | *Nano Lett.* **2010,** *10,* 4086–4092